vantages may be eclipsed by the critical problem of laser asymmetries.

The authors gratefully acknowledge the helpful suggestions and conversations with S. E. Bodner, J. Grun, M. J. Herbst, S. P. Obenschain, and B. H. Ripin at the Naval Research Laboratory. This research was supported by the U. S. Department of Energy.

[a]Present address: Berkeley Research Associates, Springfield, Va. 22150.

[1]B. H. Ripin *et al.*, Phys. Fluids 23, 1012 (1980).

[2]J. P. Anthes *et al.*, Appl. Phys. Lett. 34, 841 (1979).

[3]Y. V. Afanasêv *et al.*, Pis'ma Zh. Eksp. Teor. Fiz. 21, 150 (1975) [JETP Lett. 21, 68 (1975)].

[4]J. Nuckolls *et al.*, Nature (London) 239, 139 (1972).

[5]W. C. Mead and J. D. Lindl, Lawrence Livermore Laboratory Report No. UCRL-78459, 1976 (unpublished), and Bull. Am. Phys. Soc. 21, 1102 (1976).

[6]J. P. Boris, Naval Research Laboratory Memorandum Report No. 3427, 1976 (unpublished); J. P. Boris, Comments Plasma Phys. Controlled Fusion 3, 1 (1977).

[7]J. P. Boris and D. L. Book, Methods Comput. Phys. 16, 85 (1976).

[8]Naval Research Laboratory Laser-Plasma Interaction Group, Naval Research Laboratory Memorandum Report No. 4369, 1980 (unpublished).

[9]M. Herbst *et al.*, Bull. Am. Phys. Soc. 26, 1024 (1981).

[10]S. P. Obenschain *et al.*, Phys. Rev. Lett. 46, 1402 (1981).

[11]Mark H. Emery *et al.*, Bull. Am. Phys. Soc. 25, 947 (1980), and Naval Research Laboratory Memorandum Report No. 4500, 1981 (unpublished).

[12]J. H. Gardner and S. Bodner, Phys. Rev. Lett. 47, 1137 (1981).

[13]S. Bodner, Naval Research Laboratory Memorandum Report No. 4453, 1981 (unpublished).

[14]C. E. Max, Bull. Am. Phys. Soc. 25, 992 (1980); E. Fabre, Bull. Am. Phys. Soc. 25, 992 (1980); D. C. Slater, Bull. Am. Phys. Soc. 25, 992 (1980).

Absence of Fast Electrons in Laser-Irradiated Gas-Jet Targets

J. A. Tarvin, F. J. Mayer, D. C. Slater, Gar. E. Busch, G. Charatis, T. R. Pattinson, R. J. Schroeder, and D. Sullivan
KMS Fusion, Inc., Ann Arbor, Michigan 48106

and

D. L. Matthews
Lawrence Livermore National Laboratory, Livermore, California 94550

(Received 2 November 1981)

The x-ray spectrum emitted by a gas jet irradiated at 10^{16} W/cm^2 has been measured for laser wavelengths of 1.05 and 0.53 μm. The flux of hard x rays ($h\nu \geq 10$ keV) emitted by a gas jet is less than 0.3% of that emitted by a glass target irradiated at the same intensity. This low flux implies that less than 0.1% of the incident energy is used to heat electrons to energies greater than 10 keV.

PACS numbers: 52.25.Ps, 52.25.Fi, 52.40.Db

The aim of laser-fusion studies is to compress deuterium-tritium fuel to high density and then heat it to produce a thermonuclear reaction. The production of electrons with energies greater than 10 keV in laser-irradiated plasmas lowers the efficiency of the thermonuclear burn by limiting fuel density. The fast electrons heat the interior of an imploding target prematurely, making the fuel more difficult to compress; and they transport energy from the absorption region to the low-density expanding corona, reducing the efficiency with which absorbed energy is converted to kinetic energy of implosion. They have been studied in solid targets at laser wavelengths of 0.53,[1] 1.06,[1-4] and 10.6 μm,[5,6] and in gas targets at 10.6 μm.[7] The generation of fast electrons is usually associated with resonance absorption[1,7] but two-plasmon decay and stimulated Raman scattering (SRS)[8] are also believed to be important production mechanisms.

In an extension of a previous experiment,[9] we have studied the interaction of intense laser light with a gas jet. In contrast to all previous experiments with intensities greater than 10^{15} W/cm^2

of visible or infrared light, our experiment shows little evidence of fast electrons produced by 1.05- or 0.53-μm light.

The gas jet has properties which are desirable for investigating laser-plasma interactions. The density of neutral gas in the jet before irradiation varies smoothly and is easily characterized and highly reproducible. The high-density gas required to form a critical surface for visible light is confined to a comparatively small volume. The experimental arrangement is shown in Fig. 1. High-pressure gas expands through a small orifice into a vacuum chamber, forming a broad jet. The laser light travels upstream, ionizing and heating the gas. Some of the light is absorbed in the underdense plasma and some of it is scattered. The remaining light is absorbed or reflected at critical density, where the laser frequency $\omega_0 = 2\pi c/\lambda_0$ is equal to the electron plasma frequency, $\omega_p = (4\pi n_e e^2/m_e)^{1/2}$. Here n_e and m_e are the electron number density and mass, respectively. Hydrogen, nitrogen, neon, argon, and sulfur hexafluoride mixed with nitrogen were the target gases in the experiment. All but hydrogen, which was irradiated at 1.053 μm only, were irradiated both at 1.053 and at 0.527 μm. The laser pulse was 90 psec wide at half power and the light was focused by an $f/5$ parabolic mirror with a 75-cm focal length. At best focus, 90% of the light was contained in a 100-μm-diam spot, so that an 8-J pulse provided a range of intensity around 10^{15} W/cm^2.

The density profile of the gas jet is determined from interferograms of un-ionized gas and from images of harmonics of incident 1.05-μm light which are generated in the plasma. The second harmonic is emitted at critical density and the three-halves harmonic at one-fourth of critical density.[10] The molecular density produced by a 100-μm-diam orifice with a 130-atm source pressure is plotted in Fig. 2. The solid line is the Abel inversion of an interferogram of neutral nitrogen. The data points are from harmonic images. The inset shows harmonic emission from a hydrogen target. The fact that the data from ionized hydrogen match the data from ionized and un-ionized nitrogen so well verifies that the molecular density is the same for different gases and that nitrogen is fully ionized by the laser pulse. The density profile is characterized by the scale length for density variation at critical density, $L = (\rho/|\nabla\rho|)_{\rho=\rho_{crit}}$. The scale length increases with increasing orifice diameter and source pressure. It also increases as the number of electrons per molecule in the target gas increases. In this experiment, the scale length was usually about 100 μm, but it ranged from 70 to 200 μm.

The harmonic emission is weak. Less than 10^{-5} of incident 1.05-μm light is converted to the harmonics in hydrogen targets and even less is converted in nitrogen. The three-halves harmonic is usually more intense than the second harmonic, and they both become less intense when the scale length is increased. Harmonics of 1.053-μm

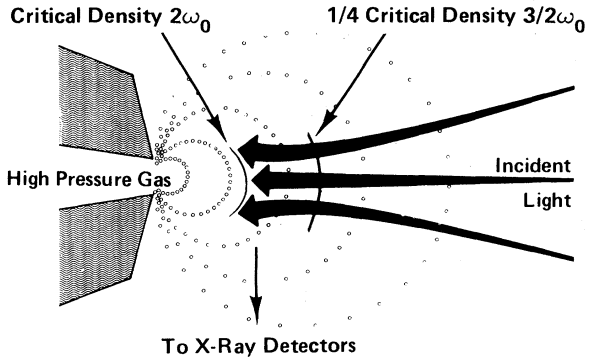

FIG. 1. The gas-jet experiment. Incident light travels up the density gradient. X-ray detectors are orthogonal to the jet axis.

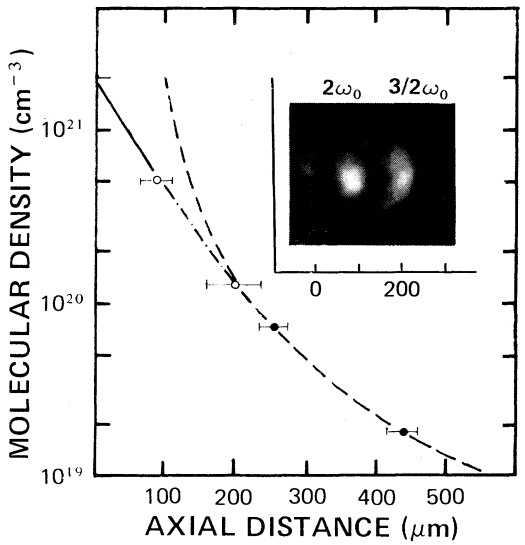

FIG. 2. Density profile of a gas jet. The solid line is from an interferogram of neutral nitrogen. Open circles, harmonic emission from hydrogen; filled circles, harmonic emission from nitrogen. The dashed line is a $1/r^2$ fit to the last three data points. Inset shows harmonic emission from hydrogen.

light were only observed from hydrogen and nitrogen and harmonics of 0.53 μm were not observed at all. In each case, the threshold for observation was about 5×10^{-9} of the incident energy.

Two techniques are used to determine the electron temperature in the plasma. At array of filtered thermoluminescent dosimeters measures the bremsstrahlung spectrum of subkiloelectronvolt x rays emitted by the jet.[11] The inferred temperature is about 500 eV and is almost independent of laser intensity. A crystal spectrograph measures the ratio of line emission from He-like and H-like species of neon, argon, and SF_6.[11,12] This diagnostic indicates that the temperature is as high as 900 eV and that the scale length for variation of temperature is hundreds of micrometers. Both of these techniques average over the whole plasma and over the whole time that the plasma emits x rays.[13] Consequently, the temperature in the absorption region is likely to be 1 keV, or slightly higher, during the peak of the laser pulse. A peak temperature of 2 keV would be inconsistent with the data.

It is difficult to study fast electrons from a laser plasma directly because high electrostatic potentials produced in the plasma alter the spectrum of electrons leaving the plasma. However, the bremsstrahlung spectrum of hard x rays gives information on the energy distribution of electrons. We measure the x-ray spectrum with an array of eight silicon p-i-n diodes with matching absorption-edge filters. The absorption edges range from 4 to 25 keV. The same array was previously used with an additional, high-energy channel in a wavelength-scaling study of spherical glass targets.[1] In that experiment, the data were fitted successfully with a two-temperature bremsstrahlung model. The cold-electron temperature θ_c was 1 keV, typically, and the hot-electron temperature θ_h varied between 4 and 20 keV, depending on intensity and wavelength. The hard-x-ray spectrum $dE_{rad}/dh\nu$ obtained from an argon gas-jet target is compared with that from a glass target in Fig. 3. In both cases, the incident wavelength is 0.53 μm, the pulse length is 90 psec, the laser energy is about 60 J, and the intensity is about 8×10^{15} W/cm^2. Thermoluminescent dosimeters show that the total x-ray emission from one target is about the same as from the other. The Ar target has a lower temperature, however, and so its spectrum falls more rapidly between 3 and 10 keV. Above 10 keV the x-ray flux from Ar is weak (three of the four data points are consistent with zero) and we can only place

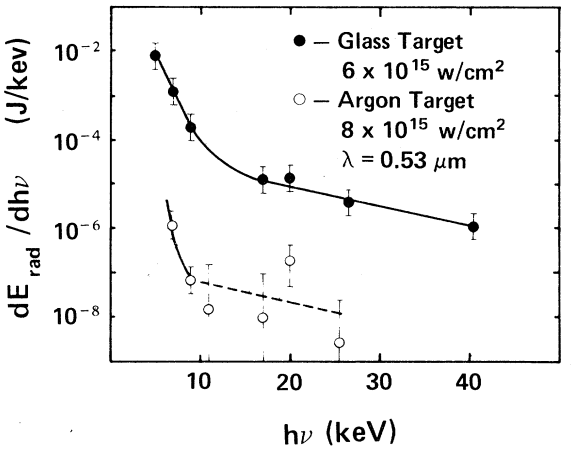

FIG. 3. Hard-x-ray spectra for glass and gas-jet targets with similar laser energy, intensity, and pulse length. Curves are best fits by a two-temperature bremsstrahlung spectrum. Dashed line is obtained with θ_h fixed at 12 keV.

an upper limit on $dE_{rad}/dh\nu$. If θ_h is the same for the Ar target as for the glass target (12 keV), then the spectral density from Ar is less than 0.3% of that from the glass. This limit is only weakly dependent on the assumed θ_h. Below 10 keV, the x-ray spectrum depends upon laser wavelength and target gas; but, above 10 keV, the spectrum is similar to the Ar spectrum for both wavelengths and all target gases.

The total energy E_h of suprathermal electrons generated in a laser target can be estimated from the bremsstrahlung spectrum. By assuming that fast electrons lose most of their energy in collisions with thermal electrons, Brueckner[14] was able to relate E_h to the x-ray spectral density at zero energy $(dE_{rad}/dh\nu)_{h\nu=0}$. Brysk[15] noted, correctly, that $(dE_{rad}/dh\nu)_{h\nu=0}$ cannot be measured and may not be finite. He suggested that E_h be related to the total bremsstrahlung emission E_{rad}. For a single electron with energy ϵ much greater than the plasma temperature, the ratio of the rate of bremsstrahlung emission $d\epsilon_{rad}/dx$ to the rate of collisional energy loss $d\epsilon/dx$ is[16]

$$R=-\frac{8}{3\pi}\left(\frac{e^2}{\hbar c}\right)\frac{Z}{m_e c^2}\frac{\epsilon}{\ln\Lambda}, \tag{1}$$

where Z is the ion charge state. The total energy radiated by an electron with an initial energy ϵ_0 is, therefore,

$$\epsilon_{rad}=\int_{\epsilon_0}^{0} R\,d\epsilon=\frac{4}{3\pi}\left(\frac{e^2}{\hbar c}\right)\frac{Z\epsilon_0^{\,2}}{m_e c^2\ln\Lambda}. \tag{2}$$

When this expression is averaged over a Max-

wellian distribution of N electrons with a temperature θ_h, we obtain the total hard-x-ray energy E_{rad} radiated by the target. Using[15] $\ln\Lambda = 9$, we can solve for N and calculate the total energy in fast electrons,

$$E_h = 3N\theta_h/2 = 6\times10^5 E_{rad}/(Z\theta_h/\mathrm{keV}). \quad (3)$$

This expression gives E_h in terms of parameters (E_{rad} and θ_h) which are readily obtained from computer fits of the x-ray spectra. When Eq. (3) is applied to x-ray spectra from glass targets, such as that shown in Fig. 3, we find that 8% to 15% of the incident energy is converted to fast electrons. This estimate accounts for about half the energy absorbed through resonance absorption.[1] For the Ar spectrum shown in Fig. 3, E_{rad} is 2 μJ, Z is 18, and E_h is 6 mJ. *Note that this is an upper limit and that it is only 0.01% of the incident energy.* For other targets, which have lower Z, the upper limit can be as high as 0.2%.

Why is there such a dramatic reduction of fast electrons? The most important mechanism for producing fast electrons in the glass target is resonance absorption, which would be eliminated in the gas jet if stimulated Brillouin scattering or collisional (inverse bremsstrahlung) absorption prevented light from reaching critical density. Strong backscatter occurs[17] at both laser wavelengths, but the scattered energy is never more than about half the incident, so that stimulated Brillouin scattering alone would not prevent light from reaching critical density. For a plasma with a 100-μm scale length and a 1-keV electron temperature, collisional absorption[18] can significantly reduce the intensity of 1.05-μm light reaching critical density if Z is greater than five. The absorption is more complete for higher Z, greater scale length, and shorter wavelength. This functional dependence is entirely consistent with the variation of the intensity of second-harmonic emission observed in this experiment. A hydrogen gas jet with a 100-μm scale length, however, should only have collisional absorption very near critical density. The large scale length must be inhibiting resonance absorption directly in this case; otherwise, the second-harmonic emission would be much more intense than it is.

Two-plasmon decay is another possible source of fast electrons, but, even when two-plasmon decay has been observed,[6] it has not been particularly strong, and so the fact that it does not produce an observable number of fast electrons in gas jets is not a great surprise. On the other hand, one might have expected SRS to produce fast electrons in gas-jet targets. For an incident wavelength of 0.53 μm, we searched for backscattered light in the range from 0.57 to 1.1 μm. A broad spectrum in that range would be the result of SRS. Weak scattering was observed below 0.6 μm, but this feature was probably an artifact induced by the very strong signal at 0.53 μm. From 0.6 to 1.1 μm, no light was observed. For wavelengths less than 0.9 μm, the detection threshold was 10^{-8} of the intensity of scattered 0.53-μm light. From 0.9 to 1.1 μm, the threshold gradually increased to 10^{-5}. So, SRS was also weak.

Gas jets have an uncommonly benign response to intense laser radiation. This response is related to the weak density gradients present in the plasma, which tend to enhance collisional absorption and stimulated Brillouin scattering at the expense of resonance absorption.

We are grateful to D. Mitrovich, T. Speziale, R. L. Berger, and T. W. Johnston for discussions which improved the interpretation of these experiments. This work was performed under U. S. Department of Energy Contract No. DE-AC08-78DP40030.

[1]D. C. Slater, Gar. E. Busch, G. Charatis, R. R. Johnson, F. J. Mayer, R. J. Schroeder, J. D. Simpson, D. Sullivan, J. A. Tarvin, and C. E. Thomas, Phys. Rev. Lett. 46, 1199 (1981).

[2]R. A. Haas, W. C. Mead, W. L. Kruer, D. W. Phillion, H. N. Kornblum, J. D. Lindl, W. L. Kruer, V. C. Rupert, and K. G. Tirsell, Phys. Fluids 20, 322 (1977).

[3]J. D. Hares, J. D. Kilkenny, M. H. Kay, and J. G. Lumey, Phys. Rev. Lett. 42, 1216 (1979).

[4]D. W. Forslund, J. M. Kindel, and K. Lee, Phys. Rev. Lett. 39, 284 (1977).

[5]D. V. Giovanielli, J. F. Kephart, and A. H. Williams, J. Appl. Phys. 47, 2907 (1976).

[6]N. A. Ebrahim, H. A. Baldis, C. Joshi, and R. Benesch, Phys. Rev. Lett. 45, 1179 (1980).

[7]P. Kolodner and E. Yablonovich, Phys. Rev. Lett. 37, 1754 (1976).

[8]M. Bornatici, J. Plasma Phys. 14, 105 (1975).

[9]F. J. Mayer, Gar. E. Busch, C. M. Kinzer, and K. Estabrook, Phys. Rev. Lett. 44, 1498 (1980).

[10]A. V. Vinogradow and V. V. Pustovalov, Zh. Eksp. Teor. Fiz. 63, 940 (1972) [Sov. Phys. JETP 36, 492 (1973)]; Paul A. Koch and J. Albritton, Phys. Rev. Lett. 34, 1616 (1975).

[11]G. Charatis *et al.*, in *Low Energy X-ray Diagnostics—1981*, edited by D. T. Attwood and B. L. Henke, AIP Conference Proceedings No. 75 (American Institute of Physics, New York, 1981), p. 270.

[12]D. L. Matthews *et al.*, Bull. Am. Phys. Soc. 26, 817 (1981), and to be published.
[13]D. Mitrovich, private communication.
[14]K. A. Brueckner, Phys. Rev. Lett. 36, 677 (1976).
[15]H. Brysk, Phys. Rev. Lett. 37, 1242 (1976).
[16]J. D. Jackson, *Classical Electrodynamics* (Wiley, New York, 1962), p. 513.
[17]J. A. Tarvin *et al.*, KMS Fusion Annual Technical Report, 1980 (unpublished), Sec. 2.2.
[18]K. R. Lang, *Astrophysical Formulae* (Springer-Verlag, New York, 1974), p. 56; P. J. Catto and T. Speziale, Phys. Fluids 20, 167 (1977).

Test-Particle Transport in Stochastic Magnetic Fields: A Fluid Representation

Harvey A. Rose
Los Alamos National Laboratory, Los Alamos, New Mexico 87545
(Received 28 September 1981)

The enhancement of diffusion perpendicular to a strong magnetic field, induced by low-amplitude field fluctuations, is calculated. A novel fluid representation of a model Fokker-Planck transport equation is used to show the equivalence of the above problem to that of a passive scalar advected by a prescribed fluctuating velocity field.

PACS numbers: 52.25.Fi, 52.25.Gj

A charged test particle which suffers collisions with a background thermal plasma, and is under the influence of a strong uniform magnetic field $\vec{B}_0$ ($\omega_c\tau \gg 1$, where ω_c is the gyrofrequency and τ the collision time), is known to have a parallel diffusion coefficient $D_\parallel$ which greatly exceeds the perpendicular diffusion coefficient $D_\perp$, $D_\perp/D_\parallel \sim \epsilon^2$, where $\epsilon = 1/\omega_c\tau$. When a small-amplitude fluctuating component, $\delta\vec{B}$, is added to $\vec{B}_0$ such that the resulting field line trajectories are stochastic, i.e., they have a perpendicular component $\vec{r}_\perp$ which diffuses,

$$\lim_{s\to\infty} \vec{r}_\perp^{\,2} = 2D_m s,$$

where s is arc length along a field line and D_m is the magnetic diffusivity, it is known that $D_\perp(\delta\vec{B})$ no longer goes to zero with ϵ. For the special case of frozen (time independent) $\delta\vec{B}$, and in the collisionless limit [$V_T\tau \gg L_k$, where V_T is the thermal speed and L_k is the exponentiation length for the separation, Δ, of neighboring magnetic field lines, $\Delta \sim \exp(s/L_k)$] Rechester and Rosenbluth[1] (RR) have estimated $D_\perp = D_m V_T$.

The purpose of this Letter is to quantify and extend the analysis of RR to the case of small-amplitude, homogeneous, but otherwise arbitrary magnetic field fluctuations and a distribution of test particles with arbitrary initial spatial variation. This is done by an approximate analysis of a model stochastic transport equation in the test-particle phase space, of a kind similar to that used by Krommes, Kleva, and Oberman.[2]

Let $\vec{b} = \vec{B}/|\vec{B}|$ ($|\vec{B}| = B_0 = \text{const}$) be written as

$$\vec{b} = \vec{e}_1(1 - h^2/2) + h_2(\vec{x}, t)\vec{e}_2 + h_3(\vec{x}, t)\vec{e}_3 \equiv \vec{b}_0 + \vec{h} + O(h^2),$$

where $h^2 = h_2^2 + h_3^2 \ll 1$, $\nabla\cdot\vec{h} = O(h^2)$, $\vec{e}_1, \vec{e}_2, \vec{e}_3$ are an orthonormal triad, $\vec{e}_3 = \vec{e}_1\times\vec{e}_2$, and h_2 and h_3 are zero-mean, random variables. The model transport equation for the test-particle phase-space density, $f(\vec{x}, \vec{v}, t)$, is of the Fokker-Planck form

$$\frac{\partial f}{\partial t} + \vec{v}\cdot\frac{\partial f}{\partial \vec{x}} + \omega_c(\vec{v}\times\vec{b})\cdot\frac{\partial f}{\partial \vec{v}} = \frac{\partial}{\partial \vec{v}}\cdot\frac{V_T^2\,\partial f/\partial \vec{v} + \vec{v}f}{\tau}. \quad (1a)$$

Note that this model conserves the number of test particles, but not energy or momentum. Given the statistics of h_2 and h_3, and the initial condition for f,

$$f(\vec{x}, \vec{v}, 0) = \rho(\vec{x})(\exp -\vec{v}^{\,2}/2V_T^2)/(2\pi V_T^2)^{3/2}, \quad (1b)$$

we can find $\rho(\vec{x}, t) = \int f(\vec{x}, \vec{v}, t)d^3v$, the spatial density of particles. On general grounds it is expected that ρ will satisfy a diffusion equation as $t\to\infty$. If $\vec{b}$ is a constant, the diffusion tensor can be calculated by standard methods. But when $\vec{b}$ fluctuates, one usually conceives of first finding an effective transport equation for $\langle f\rangle$ and then using, for example, the Chapman-Enskog procedure to determine the diffusion of $\langle\rho\rangle$. Instead, we will derive a fluctuating hydrodynamic representation for (1), and directly calculate $\langle\rho\rangle$.

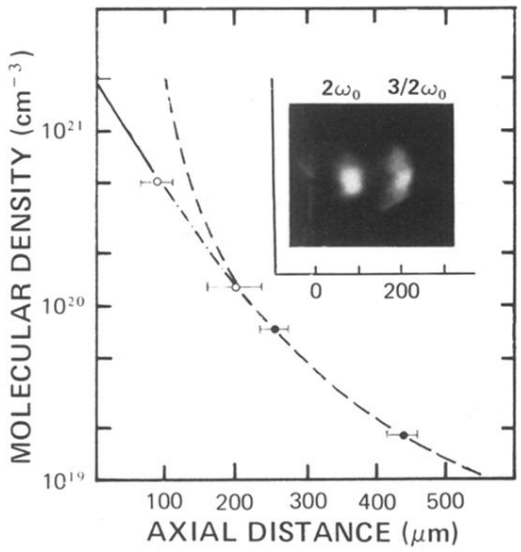

FIG. 2. Density profile of a gas jet. The solid line is from an interferogram of neutral nitrogen. Open circles, harmonic emission from hydrogen; filled circles, harmonic emission from nitrogen. The dashed line is a $1/r^2$ fit to the last three data points. Inset shows harmonic emission from hydrogen.